Conduction-band electronic states of $YbInCu_4$ studied by photoemission and soft x-ray absorption spectroscopies

Yuki Utsumi,[1,*] Hitoshi Sato,[2,†] Hidenao Kurihara,[1] Hiroyuki Maso,[1] Koichi Hiraoka,[3] Kenichi Kojima,[4] Komei Tobimatsu,[1] Takuo Ohkochi,[5,‡] Shin-ichi Fujimori,[5] Yukiharu Takeda,[5] Yuji Saitoh,[5] Kojiro Mimura,[6] Shigenori Ueda,[7] Yoshiyuki Yamashita,[7] Hideki Yoshikawa,[7] Keisuke Kobayashi,[7] Tamio Oguchi,[8] Kenya Shimada,[2] Hirofumi Namatame,[2] and Masaki Taniguchi[1,2]

[1]*Graduate School of Science, Hiroshima University, Higashi-Hiroshima 739-8526, Japan*
[2]*Hiroshima Synchrotron Radiation Center, Hiroshima University, Higashi-Hiroshima 739-0046, Japan*
[3]*Graduate School of Science and Engineering, Ehime University, Matsuyama 790-8577, Japan*
[4]*Graduate School of Integrated Arts and Sciences, Hiroshima University, Higashi-Hiroshima 739-8521, Japan*
[5]*Synchrotron Radiation Research Center, Japan Atomic Energy Agency, Hyogo 679-5148, Japan*
[6]*Graduate School of Engineering, Osaka Prefecture University, Sakai 599-8531, Japan*
[7]*NIMS Beamline Station at SPring-8, National Institute for Materials Science, Hyogo 679-5148, Japan*
[8]*ISIR, Osaka University, Ibaraki 567-0047, Japan*

(Received 7 April 2011; revised manuscript received 3 August 2011; published 26 September 2011)

We have studied conduction-band (CB) electronic states of a typical valence-transition compound $YbInCu_4$ by means of temperature-dependent hard x-ray photoemission spectroscopy (HX-PES) of the Cu $2p_{3/2}$ and In $3d_{5/2}$ core states taken at $h\nu = 5.95$ keV, soft x-ray absorption spectroscopy (XAS) of the Cu $2p_{3/2}$ core absorption region around $h\nu \sim 935$ eV, and soft x-ray photoemission spectroscopy (SX-PES) of the valence band at the Cu $2p_{3/2}$ absorption edge of $h\nu = 933.0$ eV. With decreasing temperature below the valence transition at $T_V = 42$ K, we have found that (1) the Cu $2p_{3/2}$ and In $3d_{5/2}$ peaks in the HX-PES spectra exhibit the energy shift toward the lower binding-energy side by ~40 and ~30 meV, respectively, (2) an energy position of the Cu $2p_{3/2}$ main absorption peak in the XAS spectrum is shifted toward higher photon-energy side by ~100 meV, with an appearance of a shoulder structure below the Cu $2p_{3/2}$ main absorption peak, and (3) an intensity of the Cu L_3VV Auger spectrum is abruptly enhanced. These experimental results suggest that the Fermi level of the CB-derived density of states is shifted toward the lower binding-energy side. We have described the valence transition in $YbInCu_4$ in terms of the charge transfer from the CB to Yb 4*f* states.

DOI: 10.1103/PhysRevB.84.115143 PACS number(s): 75.30.Mb, 71.27.+a, 82.80.Pv, 71.20.Eh

I. INTRODUCTION

A valence transition is one of the most fascinating phenomena observed in the strongly correlated 4*f*-electron systems.[1] Although rare-earth ions generally exist in a trivalent state in compounds, Sm, Eu, Tm, and Yb ions are often in a divalent state, while Ce ions are in a tetravalent state. Among them, $YbInCu_4$ is known as a typical material exhibiting the first-order valence transition at the critical temperature of $T_V = 42$ K.[2–4] The magnetic susceptibility follows the Curie-Weiss behavior in the high-temperature (HT) phase above T_V and the effective magnetic moment is estimated to be 4.64 μ_B/Yb,[5] indicating the Yb valence (z) close to 3. The susceptibility abruptly decreases in the low-temperature (LT) phase below T_V and shows the Pauli paramagnetic behavior. The lattice parameter expands by 0.15% below T_V with the unchanged C15b-type crystal structure.[6] The lattice expansion is derived from an increase of the number of the Yb^{2+} ions, the ionic radius of which is larger than that of the Yb^{3+} ions by 10%. It indicates that the Yb valence is reduced to $z \sim 2.9$ in the LT phase. Such a slight change of the electronic states causes a drastic change in the magnetic property from nonzero magnetic moment in the HT phase to no magnetic moment in the LT phase. The Kondo temperature (T_K) gives a measure of the hybridization strength between the conduction-band (CB) and Yb 4*f* states (*c*-*f* hybridization), and it is also related to the magnitude of the local magnetic moment. The T_K value in the HT phase is estimated to be ~25 K, while T_K further increases to $T_K \sim 400$ K in the LT phase.[7] In the LT phase, as the *c*-*f* hybridization is increased, namely, T_K is high, and the local magnetic moment is fully screened by the conduction-electron spin due to the spin-spin interaction.

A large number of studies for $YbInCu_4$ based on photoemission spectroscopy (PES) have been carried out mainly focusing on a change of the Yb 4*f* electronic states between the HT and LT phases. Recent progress in the field of hard x-ray PES (HX-PES) at several keV,[8] which has widely been recognized as a powerful method to investigate the bulk electronic states, enables us to detect more sharply the valence transition as a tremendous change of the Yb 3*d* core HX-PES spectra.[9,10] We have evaluated the Yb valences to be $z \sim 2.90$ in the HT phase and $z \sim 2.75$ in the LT phase from the Yb^{2+} and Yb^{3+} structures in the Yb 3*d* HX-PES spectra measured at $h\nu = 5.95$ keV.[9]

In contrast to the clear change of the Yb-derived electronic states, a behavior of the CB electronic states across the valence transition has not fully been clarified so far, although the CB states should also contribute to the valence transition together with the Yb 4*f* states. In the present study, we have attempted to detect how the CB states behave across the valence transition in $YbInCu_4$, by means of HX-PES at $h\nu = 5.95$ keV for the Cu $2p_{3/2}$ and In $3d_{5/2}$ core states. We have also carried out soft x-ray absorption spectroscopy (XAS) in the Cu $2p_{3/2}$ core absorption region ($h\nu \sim 935$ eV) and soft x-ray PES (SX-PES) in the valence-band region excited at the Cu $2p_{3/2}$ absorption edge ($h\nu = 933.0$ eV). The

spectral changes accompanying the valence transition have successfully been observed in $YbInCu_4$ as well as the Y-doped system $Yb_{0.9}Y_{0.1}InCu_4$ with a lower transition temperature of $T_V = 25$ K.[11] We discuss the behavior of the CB states at the valence transition in $YbInCu_4$ based on these experimental results.

II. EXPERIMENT

The Cu $2p_{3/2}$ and In $3d_{5/2}$ HX-PES experiments for $YbInCu_4$ and $Yb_{0.9}Y_{0.1}InCu_4$ were carried out at the x-ray undulator beamline BL15XU of SPring-8. Synchrotron radiation was monochromatized to 5.95 keV with a Si (111) double-crystal monochromator and a post Si (333) channel-cut monochromator.[12] The HX-PES spectra were taken by using a high-energy-resolution hemispherical photoelectron analyzer (VG Scienta R4000). The total energy resolution was set to 150 meV.

The Cu $2p_{3/2}$ XAS and valence-band SX-PES at the Cu $2p_{3/2}$ absorption edge of $h\nu = 933.0$ eV were performed at the soft x-ray undulator beamline BL23SU of SPring-8.[13,14] The XAS spectra were obtained with the total-electron-yield method by detecting photocurrent from the samples with the energy resolution of 80 meV. The angle-integrated SX-PES spectra were collected by using a hemispherical photoelectron analyzer (Gammadata Scienta SES-2002). The total energy resolution was set to 100 meV.

The binding energy of the HX- and SX-PES spectra is defined relative to the Fermi level (E_F), calibrated with the Fermi edge of Au-film spectra. The Yb 3*d* HX-PES spectra and valence-band SX-PES spectra are fully consistent with our earlier works[9,15] with respect to the spectral feature and temperature dependence.

$YbInCu_4$ and $Yb_{0.9}Y_{0.1}InCu_4$ single crystals were grown by the flux method similar to that described by Sarrao *et al.*[16] Clean surfaces of the samples were obtained *in situ* by fracturing. All the experiments were carried out within the temperature range of 150–20 K and only measured on the first cooling through the valence transition in order to prevent defect formation in the sample[17,18] by repeated passing through the transition.[16]

III. RESULTS AND DISCUSSION

The PES spectra of the core states are sensitive to the change of CB states around the specific elements and the position of E_F, which provide us with useful information on the behavior of the CB states across the valence transition.[19] Figure 1 shows the temperature dependence of the Cu $2p_{3/2}$ HX-PES spectra of $YbInCu_4$ measured at 94, 72, 51, 40, and 27 K. As the lifetime broadening of the Cu 2*p* level is the narrowest among the Cu core levels, we expect that the Cu 2*p* spectrum is the most suitable for examining the chemical shift derived from the change of the CB states around the Cu site across T_V. The inset of Fig. 1 exhibits a Cu 2*p* spectrum in the wide binding-energy range. The Cu $2p_{3/2}$ and Cu $2p_{1/2}$ peaks are located at 932.84 and 952.67 eV, respectively. Weak and broad structures around 947 and 966 eV, shown by vertical bars, originate from the plasmon excitations accompanying the $2p_{3/2}$ and $2p_{1/2}$ photoemissions, respectively.

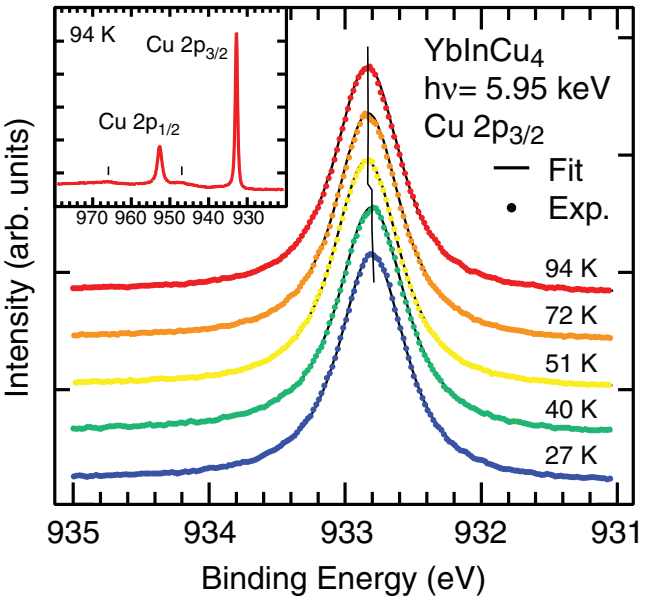

FIG. 1. (Color online) Temperature dependence of the Cu $2p_{3/2}$ HX-PES spectra of $YbInCu_4$ measured with the excitation energy of $h\nu = 5.95$ keV. Thin solid lines are fits using single line spectrum convoluted with the Lorentzian and Gaussian functions. One notices that the Cu $2p_{3/2}$ peak is abruptly shifted between 51 and 40 K across T_V toward the lower binding-energy side by ~40 meV. The inset shows the whole region of the Cu 2*p* HX-PES spectrum at 94 K. Weak and broad structures shown by vertical bars are due to the plasmon excitations accompanying the $2p_{3/2}$ and $2p_{1/2}$ photoemissions. No satellite structure is observed.

We find no satellite structure in the higher binding-energy region of the $2p_{3/2}$ and $2p_{1/2}$ peaks. As is well known, an existence of the satellite structure in the Cu 2*p* spectrum is recognized as a fingerprint for valence states of the Cu ion. According to the previously reported Cu $2p_{3/2}$ PES spectra of Cu_2O with an essentially filled Cu 3*d* shell ($3d^{10}$) and CuO with an open 3*d* shell ($3d^9$),[20] the $2p_{3/2}$ main peak of CuO ($3d^9$) at 933.2 eV is accompanied by the satellite structure, which is assigned to the $2p^53d^9$ final states, on the higher binding-energy side at about 9 eV. The spectrum of Cu_2O ($3d^{10}$), on the other hand, has only one main peak at 932.4 eV. Absence of the satellite structure in the Cu $2p_{3/2}$ HX-PES spectrum of $YbInCu_4$, thus, indicates almost fully occupied Cu 3*d* orbitals in the crystal. The Cu 2*p* spectral feature, which is similar to that of Cu metal,[21] is not changed at all between 94 (HT phase) and 27 K (LT phase), except for the energy shift as described below.

In Fig. 1, dots represent the experimental results and thin solid lines the fitting results using a single line spectrum convoluted with the Lorentzian and Gaussian functions. Closed circles in Fig. 2 exhibit the binding-energy positions of the Cu $2p_{3/2}$ peaks evaluated by the fitting procedure as a function of temperature. The Cu $2p_{3/2}$ core level shows a sudden shift toward the lower binding-energy side by ~40 meV from 51 to 40 K across the valence transition. We should note here that E_F was carefully checked just before and after the measurements to deduce these results.

In order to confirm that the sudden energy shift is essentially related to the valence transition, we have measured the Cu 2*p*

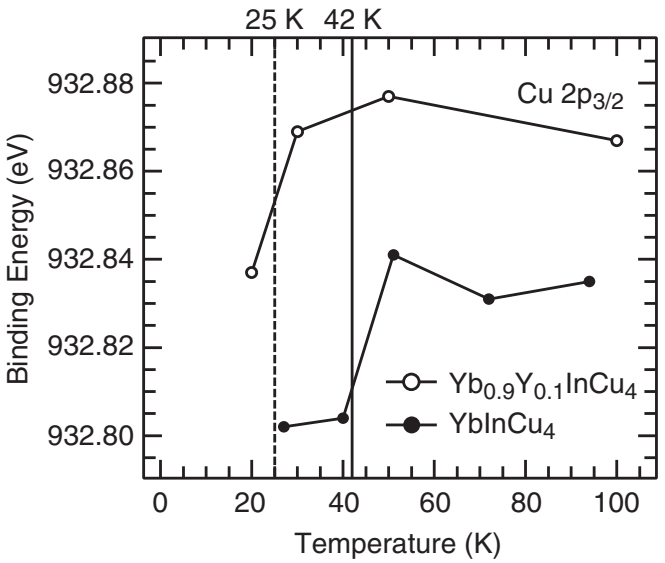

FIG. 2. Binding-energy plots of the Cu $2p_{3/2}$ peaks of $YbInCu_4$ (closed circles) and $Yb_{0.9}Y_{0.1}InCu_4$ (open circles) as a function of temperature. The abrupt energy shifts toward the lower binding-energy side are observed for both compounds with decreasing temperature across the respective valence-transition temperatures.

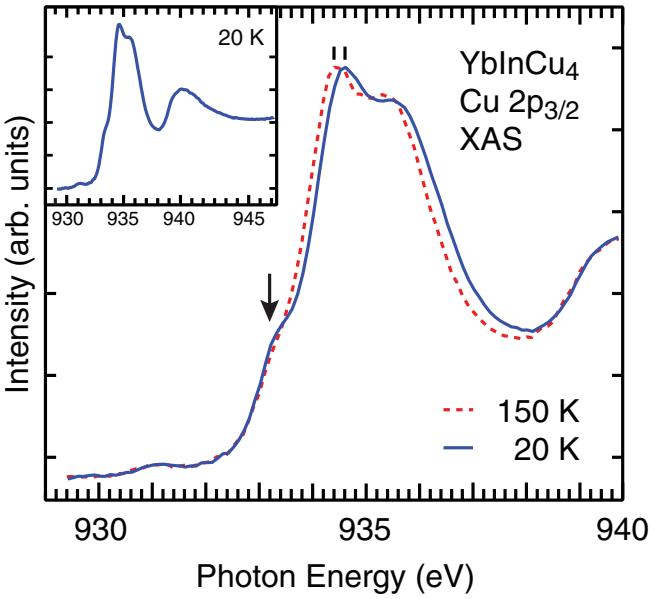

FIG. 3. (Color online) Cu $2p_{3/2}$ XAS spectra of $YbInCu_4$ measured at 150 (dashed line) and 20 K (solid line). The energy position of the main absorption peak is shifted toward the higher photon-energy side at 20 K together with the appearance of the shoulder structure below the main peak as indicated by an arrow. Inset shows the XAS spectrum at 20 K in relatively wide photon-energy region. The XAS feature is similar to that of a thin bcc-type Cu layer.

HX-PES spectra of the Y-doped system $Yb_{0.9}Y_{0.1}InCu_4$ with the lower transition temperature of $T_V = 25$ K.[11] No satellite structure is observed in the Cu $2p$ spectrum as in the case of $YbInCu_4$. Open circles in Fig. 2 show the binding-energy positions of the Cu $2p_{3/2}$ peak for $Yb_{0.9}Y_{0.1}InCu_4$ obtained by the same procedure. Note that the abrupt shift toward the lower binding-energy side by ~40 meV is also observed between 30 and 20 K across the valence transition ($T_V = 25$ K). These experimental results indicate that the CB electronic states around the Cu site are changed significantly between the HT and LT phases.

In order to further investigate the behavior of the CB electronic states around the Cu site across the valence transition, we examine the Cu $2p_{3/2}$ XAS spectra of $YbInCu_4$ taken at 150 (HT phase) and 20 K (LT phase) as shown in Fig.3. The absorption intensity is weak and the signal-to-background ratio (S/B) is about 1 as in Cu metal. The inset of Fig. 3 shows the $2p_{3/2}$ XAS spectrum at 20 K in the wide photon-energy region. There are two peak structures around 935 and 940 eV and the $2p_{3/2}$ main absorption peak around 935 eV further splits into two structures clearly at 934.6 and 935.6 eV. The XAS spectra are completely different from that of CuO ($3d^9$), where an intense peak due to the $2p^9 3d^{10}$ final states is dominant, and also from that of Cu_2O ($3d^{10}$).[22] The spectral feature is rather similar to that of the thin Cu layer with body-centered-cubic (bcc) structure with respect to the two peak structures around 935 and 940 eV,[23] apart from the splitting of the $2p_{3/2}$ main absorption peak. The present result may imply that the Cu ions occupying the 16*e* site in the C15b-type structure are bonded directly to each other as in the Cu metal. It is different from CuO and Cu_2O in which Cu ions are covalently bonded with the O ions. Ebert *et al.* compared the Cu $2p_{3/2}$ XAS spectra of the thin Cu layers with bcc structure and face-centered-cubic (fcc) structure with the theoretical calculation for the unoccupied Cu *s* and *d* partial densities of states (DOS) and found an excellent agreement between the experiments and theory.[23] According to their results, the XAS spectra of $YbInCu_4$ in the present experiments also reflect the unoccupied *s* and *d* partial DOS.

In Fig. 3, we notice that the Cu $2p_{3/2}$ XAS spectra exhibit a clear change between the HT (150 K) and LT (20 K) phases; (1) the energy position of the main absorption peak is shifted toward the higher photon-energy side by ~100 meV at 20 K, keeping the spectral feature almost unchanged, and (2) a distinct shoulder structure appears below the main peak at 20 K as indicated by an arrow in the figure. These XAS results indicate that the unoccupied DOS derived from the CB electronic states around the Cu site are substantially changed across the valence transition.

In order to observe how the Cu-derived CB states are changed at T_V, we have measured valence-band SX-PES spectra of $YbInCu_4$ at the Cu $2p_{3/2}$ absorption edge of $h\nu = 933.0$ eV. Figure 4(a) shows the valence-band SX-PES spectra of $YbInCu_4$ in the wide binding-energy region taken at 150 and 20 K. The obtained SX-PES results are in agreement with our previous results of SX-PES at $h\nu = 800$ eV.[15] The prominent peaks in the vicinity of E_F and at 1.45 eV originate from the Yb^{2+} $4f_{7/2}$ and $4f_{5/2}$ states, respectively, and the multiplet structures at 4.5–12 eV from the Yb^{3+} $4f$ states. The intensity of the Yb^{2+} (Yb^{3+})-derived structure abruptly increases (decreases) between 50 and 40 K due to the valence transition. The temperature dependence of the Cu $3d$-derived structures with the two peaks at 3.2 and 4.2 eV is negligibly small compared with that of the Yb $4f$-derived structures. No resonance enhancement in the Cu $3d$ structures is detected around the Cu $2p_{3/2}$ excitation region, in contrast to SX-PES spectra of CuO.[24] Only the Cu L_3VV Auger

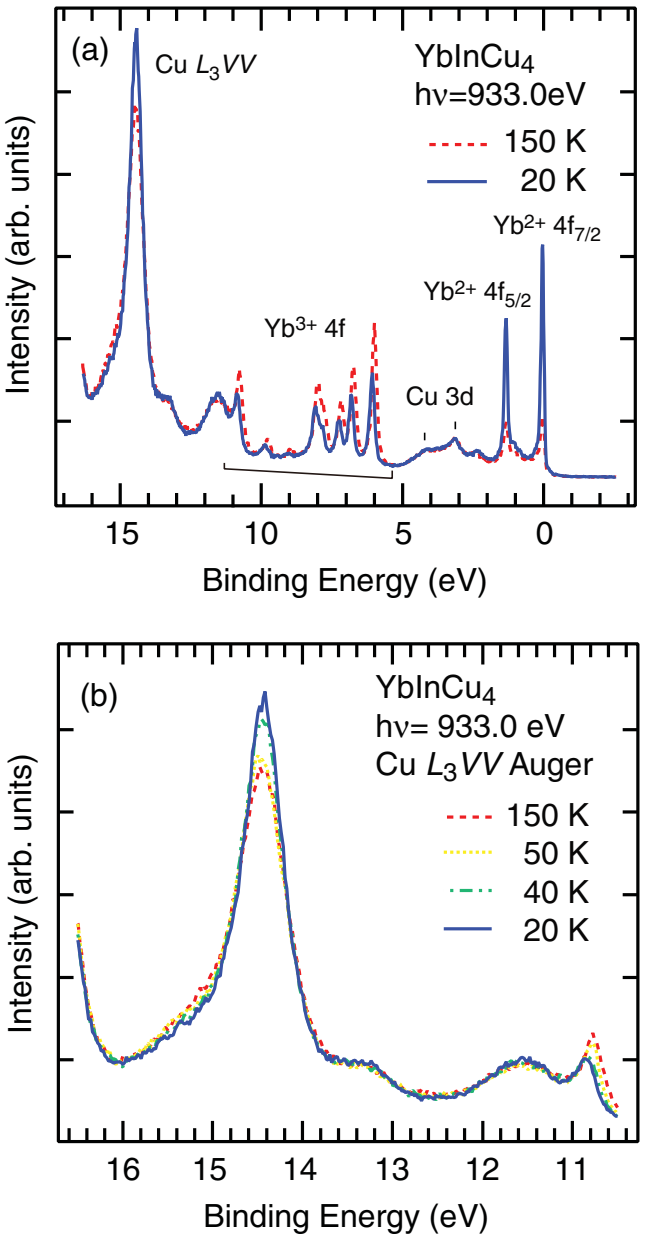

FIG. 4. (Color online) (a) Valence-band SX-PES spectra of $YbInCu_4$ at 150 and 20 K with the excitation energy of $h\nu = 933.0$ eV at the Cu $2p_{3/2}$ absorption edge. At 20 K, the Yb^{2+} $4f_{7/2}$ and $4f_{5/2}$ peaks are enhanced, while the Yb^{3+} $4f$ multiplet structures are reduced due to the valence transition. On the other hand, no change in the Cu $3d$ structures (vertical bars) is observed. The remarkable peak at 14.4 eV is ascribed to the Cu L_3VV Auger electron emission. (b) Temperature dependence of the Cu L_3VV Auger structure. The prominent peak at 14.4 eV exhibits an abrupt enhancement below T_V.

electron-originated structures are prominent with a peak at 14.4 eV and small structures at 13.2 and 11.5 eV, which is almost identical with the Cu metal.[25] These results again indicate that the Cu $3d$ states in $YbInCu_4$ are almost fully occupied, consistent with the Cu $2p_{3/2}$ HX-PES results.

Figure 4(b) shows details of the temperature dependence of the Cu L_3VV Auger-derived structure. The Auger peak at 14.4 eV is enhanced significantly between 50 and 40 K across T_V, keeping its whole feature almost unchanged. The intensity of the Auger peak is almost proportional to the absorption intensity[25] and its abrupt enhancement is considered to reflect the increase of absorption intensity at $h\nu = 933.0$ eV. The Auger spectrum of $Yb_{0.9}Y_{0.1}InCu_4$ also behaves similarly across T_V as in $YbInCu_4$.

Since the Cu $2p_{3/2}$ XAS spectra in Fig. 3 reflect the unoccupied s and d partial DOS, the appearance of the shoulder structure below the $2p_{3/2}$ absorption peak in the LT phase indicates that the unoccupied DOS are newly produced below T_V. By taking into account that the Yb valence decreases in the LT phase, it is reasonably considered that the CB electrons around the Cu site are transferred into the Yb $4f$ level at T_V leading to the valence transition in $YbInCu_4$. Since the transition into the empty Cu $3d$ states mainly contributes to the Cu $2p_{3/2}$ XAS spectra compared with that into Cu $4s$ states, we consider that the shoulder structure is derived mainly from the $3d$ states and that the Cu $3d$ electrons move into the Yb $4f$ levels at T_V.

In the XAS spectra around 933 eV, the gradient of the spectrum becomes slightly steeper at 20 K with the appearance of the shoulder structure. It indicates that the unoccupied DOS at E_F $[N(E_F)]$ increases in the LT phase, which is consistent with the experimental results of ^{63}Cu magnetic resonance studies on $YbInCu_4$.[26] The positive value of the Knight shift $K(^{63}\mathrm{Cu})$ indicates that the s electrons dominantly contribute to $K(^{63}\mathrm{Cu})$, which suggests the charge transfer also from the Cu $4s$ states to the Yb $4f$ level at T_V.

Based on the present results of the Cu $2p_{3/2}$ HX-PES, Cu $2p_{3/2}$ XAS, and Cu L_3VV Auger SX-PES taken at the Cu $2p_{3/2}$ absorption edge, here we describe the valence transition in $YbInCu_4$ in terms of the charge transfer from the CB states into the Yb $4f$ level. The CB-$4f$ charge transfer is schematically shown in Fig. 5 based on a one-electron picture for simplicity.[27] The vertical axis represents the energy relative to E_F. In the HT phase, most Yb ions are trivalent and the $4f$ orbitals have one hole. According to the band-structure calculation, E_F in the HT phase is located in the quasigap region with low DOS except for the Yb $4f$ states as shown in Fig. 5.[28] The low CB-DOS at E_F is also experimentally supported from the Hall coefficient measurements on $YbInCu_4$ and $LuInCu_4$ in comparison with $YbXCu_4$ and $LuXCu_4$ (X = Au, Zn, Cd, Mg, and Tl).[29]

With decreasing temperature across T_V, the CB electrons are transferred into the Yb $4f$ level, and then some Yb ions become divalent in the LT phase. Consequently, assuming the rigid band, the Yb $4f$ states are shifted to the higher binding-energy side and the CB-DOS to the lower binding-energy side. As the result, a higher CB-DOS is located just above E_F in the LT phase and $N(E_F)$ significantly increases because E_F moves away from the quasigap region in the HT phase to the high DOS region in the LT phase. We consider that the shoulder structure in the Cu $2p_{3/2}$ XAS spectrum at 20 K reflects the higher DOS at E_F in the LT phase. The energy shifts of the Cu $2p_{3/2}$ HX-PES and XAS spectra are also qualitatively understood from the E_F position of the CB-DOS as shown by dashed lines in Fig.5. The experimental results are, thus, well interpreted by considering the CB-$4f$ charge transfer at the valence transition.

The rigid band shift under an assumption of the CB-$4f$ charge transfer has already been suggested by Figueroa *et al.*[29] The increase of $N(E_F)$ in the LT phase enhances the c-f

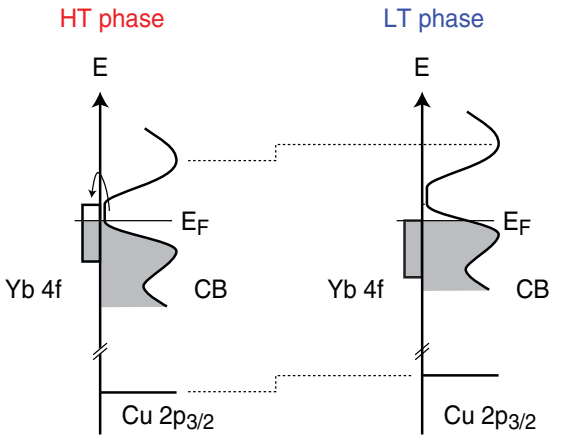

FIG. 5. (Color online) Schematic view of the CB-Yb 4*f* charge transfer at the valence transition in $YbInCu_4$. The vertical axis represents the energy relative to E_F and the Yb 4*f*- and CB-derived DOS are drawn based on a one-electron picture. In the HT phase, E_F is located in the quasigap region with the low CB-DOS. Across the valence transition, the CB electrons are transferred into the Yb 4*f* level and some Yb ions become divalent. The CB-4*f* charge transfer causes the energy shifts of the Yb 4*f*- and CB-DOS toward the opposite side. Consequently, a higher CB-DOS is located just above E_F in the LT phase and the increase of $N(E_F)$ enhances the *c*-*f* hybridization. The CB-4*f* charge transfer is observed as the energy shifts in the Cu $2p_{3/2}$ HX-PES and XAS spectra between HT and LT phases as shown by dashed lines.

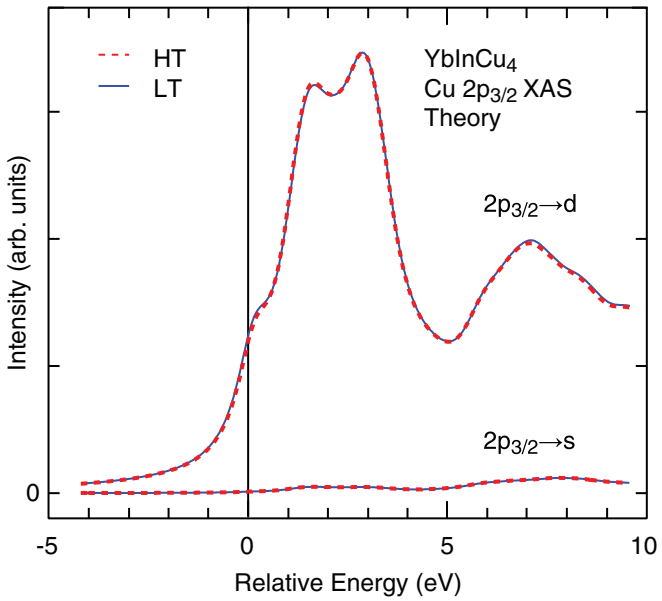

FIG. 6. (Color online) Theoretical Cu $2p_{3/2}$-*d* and $2p_{3/2}$-*s* XAS spectra for the HT (thick dashed lines) and LT (thin solid lines) phases of $YbInCu_4$ derived from the LDA calculations with the FLAPW method. The positional parameters of the Cu ions and lattice constants at 300 and 20 K are used for the calculations for the HT and LT phases, respectively. Both the $2p_{3/2}$-*d* and $2p_{3/2}$-*s* XAS features are not changed between the HT and LT phases and the LDA calculations do not interpret the change of the experimental XAS spectra (Fig. 3) due to the valence transition. The theoretical $2p_{3/2}$-*d* XAS feature is in good agreement with the experimental one at 20 K.

hybridization strength Δ, proportional to $N(E_F)$, and the Kondo temperature $T_K \sim \exp[-\varepsilon_f/(2J+1)\Delta]$, where ε_f represents an energy of the *f* level relative to E_F and $J = 7/2$. This qualitatively explains the low T_K in the HT phase (~25 K) and high T_K in the LT phases (~400 K).[7] Our results provide experimental evidence for the CB-4*f* charge transfer across T_V, which is a prerequisite for this model.[29]

In order to further examine theoretically how the electronic structure of $YbInCu_4$ changes across the valence transition, we have performed the first-principles band-structure calculations for the HT and LT phases within the local density approximation (LDA) with the full-potential linearized augmented plane-wave method, calculating the Cu $2p_{3/2}$ XAS spectra for comparison with the experimental results in Fig. 3. Recently, we have found that the positional parameter *x* of the Cu ion, which occupies the 16*e* site (*x*,*x*,*x*) in the C15b-type structure, slightly increases across the valence transition, by means of synchrotron-radiation diffraction experiments for the $YbInCu_4$ single crystal.[30] In the present calculations, we took into account these results about the *x* values as well as the lattice constants (*a*); $x = 0.62521$ and $a = 7.15952$ Å at 300 K for the HT phase and $x = 0.62538$ and $a = 7.14737$ Å at 12 K for the LT phase.

Figure 6 shows the theoretical Cu $2p_{3/2}$ XAS spectra originating from the electric dipole transitions to the unoccupied Cu *s* and *d* components. The horizontal axis is energy relative to E_F. For comparison with the experiments, the theoretical spectra have been convoluted with a Lorentzian function. We find that the XAS feature is almost determined from the transitions to the *d* components.

The theoretical Cu $2p_{3/2}$ XAS spectra are in good agreement with the experimental spectrum at 20 K (see Fig. 3) including the shoulder structure near E_F except for the relative intensity of the double peak at 2–3 eV, which suggests that the LDA results reflect the electronic structure of $YbInCu_4$ in the LT phase. However, it should be noticed that the theoretical spectra do not show significant change between the HT and LT phases. The disappearance of the shoulder structure at 150 K and the energy shift of ~100 meV between 20 and 150 K are not reproduced well by the present LDA calculation. The other theoretical partial DOS are also unchanged and the E_F position, which is located around 0.25 eV below the quasigap region, is not shifted. Therefore, the LDA results indicate that the change of the experimental XAS feature is not due to the change of the local coordination around the Cu ion (*x* value) due to the valence transition.

The LDA results in agreement with the electronic structure rather in the LT phase would reflect the itinerant character of the Yb 4*f* states in the LT phase. On the other hand, the electronic structure in the HT phase would not be interpreted within the LDA because of the localized character of the Yb 4*f* states. To describe the observed energy shift of ~100 meV, the change of the E_F position between the HT and LT phases should properly be considered. Taking into account no shoulder structure in the XAS spectrum at 150 K, the actual E_F position with respect to the quasigap region in the HT phase is expected to be closer than that of the LDA results because the

shoulder structure stems from the DOS between the quasigap region and E_F.

As is well known, LDA often does not give an accurate description of the electronic structure of the strong electron correlation systems such as the $4f$ and $5f$ ones including $YbInCu_4$, and we need to go beyond the LDA for its description. The difficulty arises from their duality between localized and itinerant characters. To this end, for example, the combination of the LDA and dynamical mean-field theory (DMFT) (LDA + DMFT) has been applied to these systems.[31,32] As regards $YbInCu_4$, Thunström *et al.* reported the Yb f-partial DOS calculated based on the LDA + Hubbard-I approximation, which combines the many-body effects for the localized atomiclike states with the one-electron picture to treat the delocalized states.[33] The theoretical result well reproduces the x-ray photoemission spectrum including the Yb^{3+} $4f$ multiplet structures. However, the temperature dependence of Yb-derived states is not elucidated based on the LDA + Hubbard-I approximation.

Burdin and Zlatić discussed the thermodynamic and transport properties of the Ce, Eu, and Yb intermetallic compounds using the periodic Anderson model with an infinite correlation between the f electrons, and reported that the behavior of these systems is determined by ratio of T_0/T_K, where T_K is again the Kondo temperature and T_0 the Fermi-liquid scale.[34] According to their discussion, the E_F position of $YbInCu_4$ is close to the quasigap region in the CB-DOS, and this situation categorizes $YbInCu_4$ to the $T_0 \gg T_K$ case, which leads to the abrupt transition from the HT phase with the local moment to the LT phase with the correlated Fermi-liquid state (see Fig. 3 in Ref. 34). In the LT phase, E_F moves out of the quasigap region and the Kondo coupling increases. From the consideration of the free energy, they also point out that T_K should be higher than T_V. Their theory thus describes the physical properties of $YbInCu_4$ qualitatively. The present results are experimental evidence for their discussion based on the E_F position of the CB-DOS. In order to reveal the mechanism of the valence transition in detail, further theoretical studies on the electronic structure of $YbInCu_4$, including the CB-DOS feature and the E_F position, are strongly required.

Finally, we briefly comment on the temperature dependence of the In $3d_{5/2}$ HX-PES spectra of $YbInCu_4$. If we consider the experimental results reflecting the rigid band shift, similar behavior should be observed in the In-related core HX-PES spectra. We find that the In $3d_{5/2}$ level of $YbInCu_4$ is actually shifted toward lower binding-energy side by ~30 meV with decreasing temperature from 51 to 40 K (not shown here) similar to the Cu $2p_{3/2}$ level shown in Fig. 2. The energy shift of the In $3d_{5/2}$ spectra across $T_V = 25$ K is also observed for the Y-doped system $Yb_{0.9}Y_{0.1}InCu_4$. These In $3d_{5/2}$ HX-PES results also support the energy shift of the E_F position in the CB-DOS across T_V.

Recently, Mimura *et al.* have measured the Pd $3d$ HX-PES spectra of $EuPd_2Si_2$ at $h\nu = 5.95$ keV,[35] where $EuPd_2Si_2$ undergoes a continuous valence transition around 160 K; the Eu valence changes from 2.2 above 230 K to 2.8 below 100 K.[36,37] They found that the Pd $3d_{5/2}$ and $3d_{3/2}$ peaks are shifted toward the higher binding-energy side by 50 meV with decreasing temperature from 300 to 20 K. By taking notice of the Eu valence in the HT and LT phases, which has the opposite behavior for the temperature dependence of the Yb valence of $YbInCu_4$, the energy shift of the Pd $3d$ levels of $EuPd_2Si_2$ is just the same phenomenon as those of the Cu $2p_{3/2}$ and In $3d_{5/2}$ levels of $YbInCu_4$. The CB-$4f$ charge transfer and the resultant shift of the E_F position in the CB-DOS therefore play an essential role in the valence transition observed in the Yb and Eu compounds.

IV. CONCLUSIONS

We have investigated the CB electronic states of $YbInCu_4$ by means of the Cu $2p_{3/2}$ and In $3d_{5/2}$ HX-PES, Cu $2p_{3/2}$ XAS, and valence-band SX-PES at the Cu $2p_{3/2}$ absorption edge. With decreasing temperature across T_V, the Cu $2p_{3/2}$ and In $3d_{5/2}$ HX-PES spectra are shifted toward the lower binding-energy side by ~40 and ~30 meV, respectively. We also find that the Cu $2p_{3/2}$ XAS spectrum is shifted toward the higher photon-energy side by ~100 meV with the appearance of the shoulder structure below the main absorption peak in the LT phase. These experimental results provide insight into the behavior of the CB states near T_V; the CB electrons move to the Yb $4f$ level with decreasing temperature across T_V and the CB-$4f$ charge transfer induces the valence transition in $YbInCu_4$. The temperature-dependent energy shifts of the Cu $2p_{3/2}$ and In $3d_{5/2}$ levels and Cu $2p_{3/2}$ XAS results can consistently be explained by the CB-$4f$ charge transfer. Assuming the rigid band shift, the high CB-DOS is located near E_F, producing the shoulder structure in the Cu $2p_{3/2}$ XAS spectrum at 20 K. The large $N(E_F)$ triggers the increases of the c-f hybridization strength and T_K, which causes the disappearance of magnetic moment in the LT phase. The present experimental results indicate that the CB-$4f$ charge transfer and the shape of the CB-DOS play an essential role in the valence transition in $YbInCu_4$.

ACKNOWLEDGMENTS

The authors are grateful to Dr. M. Arita for the band-structure calculations of $YbInCu_4$ using the WIEN2K code. The HX-PES was performed at BL15XU of SPring-8 with the approval of NIMS Beamline Station (Proposals No. 2009A4800 and No. 2009B4803), and the SX-PES and XAS with the approval of BL23SU of SPring-8 (Proposals No. 2006B3820 and No. 2007A3838).

*utsumi-yuki@hiroshima-u.ac.jp
†jinjin@hiroshima-u.ac.jp
‡Present address: Japan Synchrotron Radiation Research Institute (JASRI), SPring-8, Hyogo 679-5198, Japan.

[1] C. M. Varma, Rev. Mod. Phys. **48**, 219 (1976).
[2] I. Felner and I. Nowik, Phys. Rev. B **33**, 617 (1986).
[3] I. Felner, I. Nowik, D. Vaknin, U. Potzel, J. Moser, G. M. Kalvius, G. Wortmann, G. Schmiester, G. Hilscher, E. Gratz, C. Schmitzer, N. Pillmayr, K. G. Prasad, H. de Waard, and H. Pinto, Phys. Rev. B **35**, 6956 (1987).

[4]K. Kojima, H. Hayashi, A. Minami, Y. Kasamatsu, and T. Hihara, J. Magn. Magn. Mater. **81**, 267 (1989).
[5]B. Kindler, D. Finsterbusch, R. Graf, F. Ritter, W. Assmus, and B. Lüthi, Phys. Rev. B **50**, 704 (1994).
[6]J. M. Lawrence, G. H. Kwei, J. L. Sarrao, Z. Fisk, D. Mandrus, and J. D. Thompson, Phys. Rev. B **54**, 6011 (1996).
[7]J. M. Lawrence, S. M. Shapiro, J. L. Sarrao, and Z. Fisk, Phys. Rev. B **55**, 14467 (1997).
[8]Y. Takata, in *Very High Resolution Photoelectron Spectroscopy*, edited by S. Hüfner (Springer, Berlin, 2007), pp. 373–397.
[9]H. Sato, K. Shimada, M. Arita, K. Hiraoka, K. Kojima, Y. Takeda, K. Yoshikawa, M. Sawada, M. Nakatake, H. Namatame, M. Taniguchi, Y. Takata, E. Ikenaga, S. Shin, K. Kobayashi, K. Tamasaku, Y. Nishino, D. Miwa, M. Yabashi, and T. Ishikawa, Phys. Rev. Lett. **93**, 246404 (2004).
[10]S. Suga, A. Sekiyama, S. Imada, J. Yamaguchi, A. Shigemoto, A. Irizawa, K. Yoshimura, M. Yabashi, K. Tamasaku, A. Higashiya, and T. Ishikawa, J. Phys. Soc. Jpn. **78**, 074704 (2009).
[11]W. Zhang, N. Sato, K. Yoshimura, A. Mitsuda, T. Goto, and K. Kosuge, Phys. Rev. B **66**, 024112 (2002).
[12]K. Kobayashi, M. Yabashi, Y. Takata, T. Tokushima, S. Shin, K. Tamasaku, D. Miwa, T. Ishikawa, H. Nohira, T. Hattori, Y. Sugita, O. Nakatsuka, A. Sakai, and S. Zaima, Appl. Phys. Lett. **83**, 1005 (2003).
[13]A. Yokoya, T. Sekiguchi, Y. Saitoh, T. Okane, T. Nakatani, T. Shimada, H. Kobayashi, M. Takao, Y. Teraoka, Y. Hayashi, S. Sasaki, Y. Miyahira, T. Harami, and T. A. Sasaki, J. Synchrotron Radiat. **5**, 10 (1998).
[14]Y. Saitoh, T. Nakatani, T. Matsushita, A. Agui, A. Yoshigoe, Y. Teraoka, and A. Yokoya, Nucl. Instrum. Methods Phys. Res., Sect. A **474**, 253 (2001).
[15]H. Sato, K. Yoshikawa, K. Hiraoka, M. Arita, K. Fujimoto, K. Kojima, T. Muro, Y. Saitoh, A. Sekiyama, S. Suga, and M. Taniguchi, Phys. Rev. B **69**, 165101 (2004).
[16]J. L. Sarrao, C. D. Immer, C. L. Benton, Z. Fisk, J. M. Lawrence, D. Mandrus, and J. D. Thompson, Phys. Rev. B **54**, 12207 (1996).
[17]D. P. Moore, J. J. Joyce, A. J. Arko, J. L. Sarrao, L. Morales, H. Hochst, and Y. D. Chuang, Phys. Rev. B **62**, 16492 (2000).
[18]J. J. Joyce, A. J. Arko, L. A. Morales, J. L. Sarrao, and H. Höchst, Phys. Rev. B **63**, 197101 (2001).
[19]We comment that it is difficult to directly observe the CB states near E_F in the PES spectra since the prominent Yb^{2+} $4f_{7/2}$ peak completely screens the contributions of the CB states to the spectra in the vicinity of E_F [see Fig. 4(a)].
[20]J. Ghijsen, L. H. Tjeng, J. van Elp, H. Eskes, J. Westerink, G. A. Sawatzky, and M. T. Czyzyk, Phys. Rev. B **38**, 11322 (1988).
[21]Z. X. Shen, J. W. Allen, J. J. Yeh, J.-S. Kang, W. Ellis, W. Spicer, I. Lindau, M. B. Maple, Y. D. Dalichaouch, M. S. Torikachvili, J. Z. Sun, and T. H. Geballe, Phys. Rev. B **36**, 8414 (1987).
[22]M. Finazzi, G. Ghiringhelli, O. Tjernberg, Ph. Ohresser, and N. B. Brookes, Phys. Rev. B **61**, 4629 (2000).
[23]H. Ebert, J. Stöhr, S. S. P. Parkin, M. Samant, and A. Nilsson, Phys. Rev. B **53**, 16067 (1996).
[24]L. H. Tjeng, C. T. Chen, J. Ghijsen, P. Rudolf, and F. Sette, Phys. Rev. Lett. **67**, 501 (1991).
[25]I. Coulthard, T. K. Sham, Y.-F. Hu, S. J. Naftel, P.-S. Kim, and J. W. Freeland, Phys. Rev. B **64**, 115101 (2001).
[26]T. Koyama, M. Matsumoto, S. Wada, and J. L. Sarrao, Phys. Rev. B **63**, 172410 (2001).
[27]From a viewpoint of a many-electron picture, the occupied Yb^{3+} $4f$ states are located well below E_F, while the unoccupied ones above E_F. In the case of $YbInCu_4$, however, the $4f$ hole states should exist just above E_F as in Fig. 5, taking into account its valence transition. Since the temperature dependence of the CB-DOS related spectral features can be reasonably interpreted based on our model, we assume that Fig. 5 depicts essential parts of the electronic states.
[28]K. Takegahara and T. Kasuya, J. Phys. Soc. Jpn. **59**, 3299 (1990).
[29]E. Figueroa, J. M. Lawrence, J. L. Sarrao, Z. Fisk, M. F. Hundley, and J. D. Thompson, Solid State Commun. **106**, 347 (1998).
[30]Y. Utsumi, H. Sato, C. Moriyoshi, Y. Kuroiwa, H. Namatame, M. Taniguchi, K. Hiraoka, K. Kojima, and K. Sugimoto, Jpn. J. Appl. Phys. **50**, 05FC10 (2011).
[31]E. R. Ylvisaker, J. Kuneš, A. K. McMahan, and W. E. Pickett, Phys. Rev. Lett. **102**, 246401 (2009).
[32]B. Amadon, S. Biermann, A. Georges, and F. Aryasetiawan, Phys. Rev. Lett. **96**, 066402 (2006).
[33]P. Thunström, I. Di Marco, A. Grechnev, S. Lebègue, M. I. Katsnelson, A. Svane, and O. Eriksson, Phys. Rev. B **79**, 165104 (2009).
[34]S. Burdin and V. Zlatić, Phys. Rev. B **79**, 115139 (2009).
[35]K. Mimura, T. Uozumi, T. Ishizu, S. Motonami, H. Sato, Y. Utsumi, S. Ueda, A. Mitsuda, K. Shimada, Y. Taguchi, Y. Yamashita, H. Yoshikawa, H. Namatame, M. Taniguchi, and K. Kobayashi, Jpn. J. Appl. Phys. **50**, 05FD03 (2011).
[36]E. Kemly, M. Groft, V. Murgai, L. C. Gupta, C. Godart, R. D. Parks, and C. U. Segre, J. Magn. Magn. Mater. **47-48**, 403 (1985).
[37]G. Wortmann, K. H. Prank, E. V. Sampathkumaran, B. Perscheid, G. Schmiester, and G. Kaindl, J. Magn. Magn. Mater. **49**, 325 (1985).